

Quantum spatial superresolution by optical centroid measurements

Heedeuk Shin¹, Kam Wai Clifford Chan^{1,2}, Hye Jeong Chang^{1,3}, and Robert W. Boyd^{1,4}

¹*The Institute of Optics, University of Rochester, Rochester, NY 14627, USA*

²*Rochester Optical Manufacturing Company, Rochester, NY 14606, USA*

³*Korean Intellectual Property Office, Daejeon 302-701, Korea and*

⁴*Department of Physics, University of Ottawa, Ottawa, ON K1N 6N5, Canada**

(Dated: January 20, 2013)

Quantum lithography (QL) has been suggested as a means of achieving enhanced spatial resolution for optical imaging, but its realization has been held back by the low multi-photon detection rates of recording materials. Recently, an optical centroid measurement (OCM) procedure was proposed as a way to obtain spatial resolution enhancement identical to that of QL but with higher detection efficiency (M. Tsang, Phys. Rev. Lett. 102, 253601, 2009). Here we describe a variation of the OCM method with still higher detection efficiency based on the use of photon-number-resolving detection. We also report laboratory results for two-photon interference. We compare these results with those of the standard QL method based on multi-photon detection and show that the new method leads to superresolution but with higher detection efficiency.

PACS numbers:

The spatial resolution of optical imaging systems has traditionally been considered to be limited by the Rayleigh resolution criterion. One means of overcoming this limit [1] is to make use of the photon correlations that exist in certain quantum states of light. A specific example of such an approach is the quantum lithography (QL) proposal of Dowling and coworkers [2]. In this approach, a path-entangled state of N photons (a $N00N$ state) is used to write an interference pattern onto a recording material that responds by means of multi-photon absorption (MPA), producing N -fold-enhanced resolution as compared with a classical fringe pattern. Experimental procedures for creating $N00N$ states with up to $N = 5$ photons by means of spontaneous parametric down conversion have been reported by several groups [3–7]. Experimental demonstrations of spatial superresolution through the QL procedure have, however, been rather limited. In one approach, multi-photon absorbing (MPA) lithographic materials are mimicked by using two single-photon detectors operated in coincidence [8, 9]. In another, poly(methyl-methacrylate) was used as a MPA lithographic material for recording sub-Rayleigh interference patterns, but only when excited by intense classical light [10]. In order to realize true quantum lithography, very sensitive lithographic materials that can respond by MPA to weak quantum states of light are required. The use of time-energy-entangled multi-photons can provide significant enhancement of the MPA transition rate because of the near-zero variation in birth time [11]. There has also been some uncertainty in the trade-off between resolution enhancement and MPA enhancement [12–15]. In summary, true quantum lithography has yet to be realized because of the low MPA efficiency of available materials.

Recently, Tsang [16] proposed an “optical centroid” method for achieving spatial interferometric superresolution with much higher detection efficiency than that of

QL. Instead of using detectors that respond by MPA as in quantum lithography, an array of single-photon detectors followed by postprocessing is used. The addresses of the N detectors that fire in response to N incident photons are recorded, and the centroid of the positions of those detectors is computed. A histogram of the positions of optical centroids determined by repeated measurements is then produced. This histogram shows an interference pattern with a resolution enhancement identical to that of the QL method. If the pixel size of the detector array is much smaller than the correlation area of the entangled photons, the probability that the photons arrive at different pixels is much larger than the probability that they arrive at same pixel. For this reason, the detection efficiency of the OCM method is much higher than that of the QL method, which relies on MPA.

In this Letter, we report the results of a proof-of-principle experiment that demonstrates optical superresolution based on an improved version of Tsang’s OCM method. The improvement comes about by implementing a form of photon-number-resolving (PNR) detection, which leads to still higher efficiency than Tsang’s original proposal. The interference fringes obtained by the OCM method are found to show resolution enhancement identical to that of the QL method, but with higher detection efficiency. To the best of our knowledge, ours is the first experimental demonstration of spatial resolution enhancement using the OCM method.

We next briefly review the theory of resolution enhancement by both the OCM and QL methods. Under the one-dimensional (x) and monochromatic approximations [13], the electric field operator on the detection plane is given by

$$\hat{E}^{(+)}(x) = i\sqrt{\frac{\eta}{(2\pi)^2}} \int dq \hat{a}(q) e^{iqx}, \quad (1)$$

where $\eta = \hbar/(2\epsilon_0 c^2 T)$ with T being the normalization

time scale. Here q and x are respectively the transverse wavevector and transverse position on the detector plane. The $N00N$ state on the detector plane is given by

$$|N00N\rangle = \frac{1}{\sqrt{2N!}} \left\{ [\hat{A}^\dagger]^N + [\hat{B}^\dagger]^N \right\} |0\rangle \quad (2)$$

where \hat{A}^\dagger and \hat{B}^\dagger represent the annihilation operators of photons in modes A and B falling onto the detector plane, respectively. \hat{A}^\dagger is $(1/\sqrt{\Delta\kappa}) \int d\kappa F^*[(\kappa_A + \kappa)/\Delta\kappa] \hat{a}^\dagger(\kappa)$ with the mean x -component of wavevector $\kappa_A = \kappa_0$. Analogously, \hat{B}^\dagger has $\kappa_B = -\kappa_0$ and $\Delta\kappa$ is the uncertainty of the transverse wavevector. $F(q)$ is the normalized transverse wavevector profile of the photon packet. Note that $[\hat{A}, \hat{A}^\dagger] = [\hat{B}, \hat{B}^\dagger] = 1$ and $[\hat{A}, \hat{B}^\dagger] = 0$ for $\kappa_0 \gg \Delta\kappa$. If we set $F(q) = (1/\sqrt{\pi}) \exp(-q^2/2\Delta\kappa^2)$, the N -photon, conditional probability density for the QL method becomes

$$\begin{aligned} P_C(x) &= \langle \hat{I}(x)^N : \rangle = \left\langle [\hat{E}^{(-)}(x)]^N [\hat{E}^{(+)}(x)]^N \right\rangle \\ &= \frac{N! \eta^N \Delta\kappa^N}{\pi^N} e^{(-N\Delta\kappa^2 x^2)} [1 + \cos(2N\kappa_0 x)]. \end{aligned} \quad (3)$$

On the other hand, the probability distribution for the optical centroid is

$$\begin{aligned} P_M(X) &= \int d\xi_1 \cdots d\xi_{N-1} \left\langle : \prod_{n=1}^N \hat{I}(X + \xi_n) : \right\rangle \\ &= \frac{N! \eta^N \Delta\kappa}{\sqrt{N\pi}^{N+1}} e^{(-N\Delta\kappa^2 X^2)} [1 + \cos(2N\kappa_0 X)], \end{aligned} \quad (4)$$

where the centroid and relative-position coordinates are defined as $X = \frac{1}{N} \sum_{n=1}^N x_n$ and $\xi_n = x_n - X$ with $n = 1, \dots, N$, respectively. $P_M(X)$ is a marginal probability density. We see that they both give the same spatial resolution enhancement. However, the ratio of probabilities for the two cases is

$$\frac{P_M(x)\delta x}{P_C(x)\delta x^N} = \frac{1}{\sqrt{N}} \left(\frac{\sqrt{\pi}}{\Delta\kappa\delta x} \right)^{N-1}, \quad (5)$$

where δx is the pixel size of detector. For typical situations in which the beam size is much larger than the pixel size, one has $\Delta\kappa\delta x \ll 1$. Therefore, $P_M(X)$ can be much greater than $P_C(x)$. Note that this conclusion holds even before taking account of the greatly different detection efficiencies of single-photon and multi-photon detectors. When these differences are taken into account, the OCM method becomes even more favorable.

To provide an intuitive understanding of the tradeoffs between the QL and OCM methods, we next present an analysis based on the use of combinatorics. We suppose that the correlation area of the photon field is M times larger than the pixel size on the detector array and that N entangled photons arrive at random positions on the

detector array within this correlation area. The total number of combinations with repetition for N photons falling on M pixels is $C_{\text{total}} = (M+N-1)!/(N!(M-1)!)$. Every such case occurs with equal probability $1/C_{\text{total}}$ because of the assumption of random positions. Therefore, the more combinations a particular method has, the more efficient it is. For instance, quantum lithography requires N -photon absorption, and the number of cases of N photons falling onto the same pixel is $C_{\text{NPA}} = M$. If all N photons do not fall onto the same detector this event will be lost, leading to decreased detection efficiency. In the OCM method, however, a single-photon detector array is used, and the number of combinations of detecting N photons by N different pixels among the M pixels is $C_{\text{SPA}} = M!/(N!(M-N)!)$. For small pixel size or large correlation area ($M \gg N$), the OCM method will be much more efficient than the QL method ($C_{\text{total}} \sim C_{\text{SPA}} \gg C_{\text{NPA}}$), as Tsang predicted.

In the laboratory, however, practical concerns may preclude the pixel area from being much smaller than the correlation area. Moreover, most currently available high-sensitivity detectors are not photon-number resolving (PNR), that is, they cannot distinguish between one and several photons falling onto the detector. If more than one photon arrives at a given pixel, the single-photon detector will count this as a single event, and fewer than N detectors will register. Then the OCM protocol will discard this event, leading to decreased measurement efficiency. This loss of efficiency becomes increasingly more significant for large photon numbers N or small values of M .

Loss of efficiency due to multi-arrivals at one pixel can be eliminated by using a photon-number-resolving (PNR) detector array. Recently, PNR detectors based on superconductive nanowire technology with high quantum efficiency have been developed [17]. The PNR detector array will measure the addresses of pixels that fire as well as the number of photons at these pixels. An accurate optical centroid of the detection process can thereby be computed. The OCM method with a PNR detector array has the number of combinations with repetition for N photons falling onto the array given by $C_{\text{PNR}} = (M+N-1)!/(N!(M-1)!)$. This result indicates that the PNR detector array can use all of the cases of N photons arriving at the detector. The PNR detector array will work like a MPA detector array for $M \sim 1$ and will be almost equal to the single-photon OCM detector for $M \gg N$.

We have performed experimental studies of superresolution for two-photon interference (that is, $N = 2$) for both the QL and OCM methods. The experimental setups are the same for both cases except for the detection method, as shown in Fig. 1. A UV light beam at 400-nm wavelength is generated by second-harmonic generation of 100-fs pulses at 800-nm wavelength at repetition rate of 82 MHz and is split into two beams by a beam splitter

(BS1). A 1.5-mm-thick BBO crystal is placed in each (mutually coherent) UV beam, and spontaneous parametric down conversion occurs randomly in each crystal under type 1 collinear phase matching conditions. After blocking the pump beams using interference filters (IF), the photon number state $|\Psi\rangle$ in mode A and B is given by

$$|\Psi\rangle = |0\rangle_A|0\rangle_B + \gamma(|2\rangle_A|0\rangle_B + |0\rangle_A|2\rangle_B)/\sqrt{2} + \dots, \quad (6)$$

where γ is the probability of creating a photon pair by parametric down-conversion. At low pump power, γ is much smaller than unity, and we can thus ignore multi-pair generation proportional to higher powers of γ . The generated light is then well approximated as a two-photon $N00N$ state. This procedure for generating the 2002 state is convenient because it avoids the need for a maintaining the sensitive alignment of a Hong-Ou-Mandel setup [3]. Moreover, strong photon flux can be obtained by using long crystals or periodically poled crystals [18]. We use a second beam splitter (BS2) to combine these two beams with a small angle ($\theta \sim 0.033^\circ$) between them. To increase the collection efficiency, two spherical lenses with 10-cm focal length are located after each IF, and each spherical lens is defocused by 0.5 mm to make the correlation area larger than the pixel size. The measured correlation area has a diameter of approximately 0.5 mm.

The two detection systems were prepared using multimode fibers (MMFs) with core and cladding diameters of $62.5 \mu\text{m}$ and $125 \mu\text{m}$, respectively. For the QL case (see Fig. 1 (b)), a single MMF acting as a collector was scanned in discrete steps of $50 \mu\text{m}$ across the detection region using a motorized translation stage. The output of this fiber was split into two additional MMFs whose outputs were monitored by two single-photon detectors operating in coincidence [9]. The coincidence circuit counts how many photon pairs arrive simultaneously at the position of the input fiber, thus emulating a two-photon detector.

The OCM detection system was constructed as follows. According to the OCM proposal, the detection system should consist of a linear array of detectors each of which can respond with high sensitivity to individual incident photons. Detector arrays of this sort are not readily available. Instead, we simulated such a detection system by using two MMFs of variable separation serving as detectors, as shown in Fig. 1 (c). For a given fixed separation, this fiber pair is scanned through the detection region while coincidence counts are recorded. The coincidence circuit counts how many photons arrive simultaneously at the two spatially separated inputs. The centroid position is located at the mean position of the two fibers. This procedure is then repeated sequentially for other fiber-to-fiber separations of 125, 250, 375, 500, and $625 \mu\text{m}$. The coincidence count rates at a given centroid position are then summed for all fiber separations. In this manner we

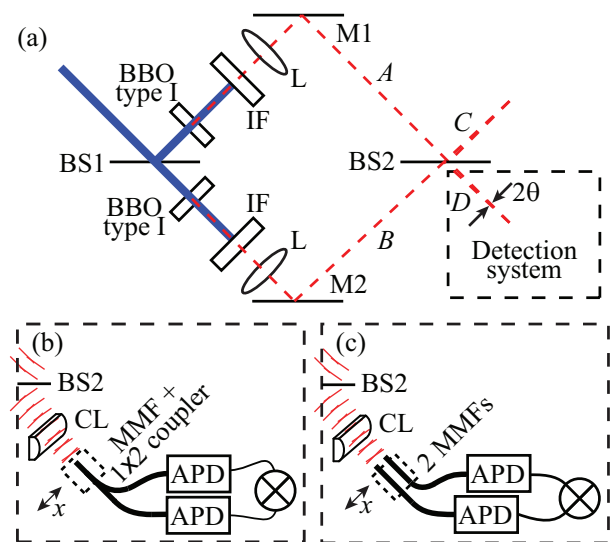


FIG. 1: (Color online) (a) Experimental setup for producing two-photon interference. The dashed lines indicate the down-converted photon-pair fluxes, and the dashed box represents the detection system used to measure the two-photon interference pattern. (b) The detection system for the QL process. A coincidence measurement that mimics two-photon absorption. (c) Detection system for the OCM procedure, as described in the text. In each case, a cylindrical lens (CL) is positioned in front of the detection systems to increase collection efficiency and the coincidence window time was 7 ns. APD = avalanche photodiode.

collect the same data that would have been collected (although more rapidly) by a multi-element detector array. To simulate a PNR detector array, we include the case of a single collection fiber coupled to two single-photon detectors (Fig. 1(b)) with that of two collection fibers of variable separation (Fig. 1(c)).

Our experimental results are shown in Fig. 2. In part (a) of the figure, we show the form of the classical, single-photon interference fringes. These results were obtained using strongly attenuated laser light of 800-nm wavelength, and serve as a reference. Under our experimental conditions, the period of these classical interference fringes was 0.69 mm. Next, two-photon interference fringes were recorded using the QL detector of Fig. 1(b). Both singles counts and coincidence counts are shown in Fig. 2(b). The singles counts show a Gaussian profile, whereas the coincidence counts exhibit an interference pattern with a decreased period of about 0.34 mm. Therefore, the QL method shows a factor-of-two increase in spatial resolution as predicted [2] and observed previously in references [8] and [9].

Next, we repeated the measurement of the two-photon spatial interference pattern using our OCM detection system. The single- and two-photon count rates for MMFs separated by $125 \mu\text{m}$ are shown in Fig. 2(c). Because of the fiber separation, the single-photon data have differ-

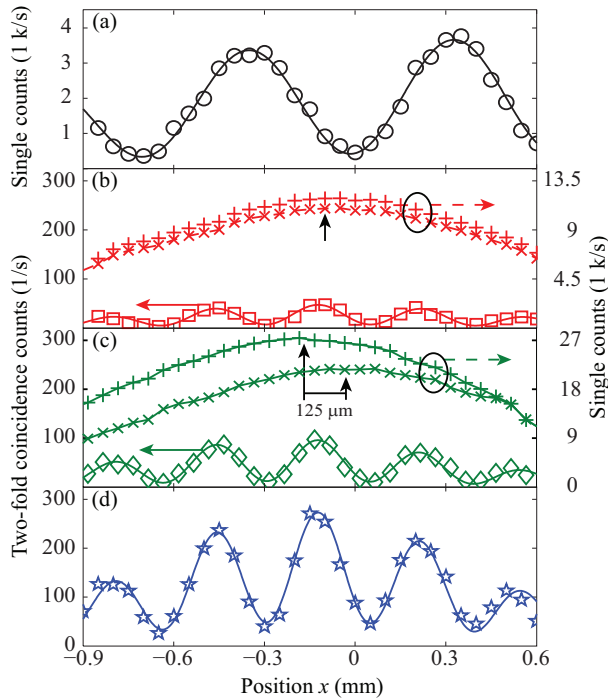


FIG. 2: (Color online) (a) Single-photon count rate for strongly attenuated coherent-state light at an 800-nm wavelength versus the detector position x . (b)-(d) Single-photon (marked + and \times) and two-photon count rates for the 2002 state as measured by (b) the QL method of Fig. 1(b), (c) the OCM method of Fig. 1(c), and (d) the OCM/PNR method described in the text. For part (c) the two parallel MMFs have a separation of $125\ \mu\text{m}$. The vertical arrows point the positions of the maximum single-photon count rates. The solid lines are theoretical fits to the data. The integration time in each case was 10 seconds.

ent peak positions separated from each other by approximately $125\ \mu\text{m}$. The period of the two-photon fringes is approximately $0.34\ \text{mm}$, the same as the QL result, demonstrating enhanced resolution by the OCM method. The fitted curve for the two-photon coincidence counts is a sinusoidal pattern weighted by a Gaussian function. Measurements of the sort shown in Fig. 2(c) were repeated for the other fiber separations. We then add all of these traces together to give the results shown in Fig. 2(d). The two-photon interference fringes obtained by the OCM method has about a 5.7-times larger fringe amplitude than the QL results. The enhancement factor depends on the value of the parameter M , which was 5.6 under our experimental conditions. Using this M value, the ratio between C_{PNR} and C_{NPA} should be 3.3, but because the coincidence detection efficiency of the QL detection system in Fig. 1(b) was reduced by half due to the 1×2 coupler, the expected enhancement factor becomes 5.6, in good agreement with the observed value. The enhancement factor will increase if one uses a detector array of smaller pixel size or if one enlarges the correlation area.

The OCM method is expected to scale well to higher values of N and thus provide still greater spatial resolution. However, the implementation studied here based on the use of N detectors of variable separation provides a highly inefficient means of scaling to higher N , because of the large number of detector configurations that must be used. Nonetheless, the results presented here provide a proof-of-principle demonstration that the OCM method for $N = 2$ can provide superresolution with a two-fold enhancement over the classical resolution limit. We have also shown that the OCM method provides the same degree of resolution enhancement as the QL method but with higher efficiency. We feel that, when large arrays of single-photon detectors become available, the OCM method will be a powerful means of providing still greater enhancement in resolution.

We thank Colin O'Sullivan for useful discussions. This work was supported by the U.S. Army Research Office through a MURI grant and by the DARPA/DSO InPho program.

* Electronic address: boyd@optics.rochester.edu

- [1] E. J. S. Fonseca, C. H. Monken, and S. Padua, *Phys. Rev. Lett.* **82**, 2868 (1999).
- [2] A. N. Boto, P. Kok, D. S. Abrams, S. L. Braunstein, C. P. Williams, and J. P. Dowling, *Phys. Rev. Lett.* **85**, 2733 (2000).
- [3] C. K. Hong, Z. Y. Ou, and L. Mandel, *Phys. Rev. Lett.* **59**, 2044 (1987).
- [4] M. W. Mitchell, J. S. Lundeen, and A. M. Steinberg, *Nature* **429**, 161 (2004).
- [5] T. Nagata, R. Okamoto, J. L. O'Brien, K. Sasaki, S. Takeuchi, *Science* **316**, 726 (2007).
- [6] P. Walther, J.-W. Pan, M. Aspelmeyer, R. Ursin, S. Gasparoni, and A. Zeilinger, *Nature* **429**, 158 (2004).
- [7] I. Afek, O. Ambar, and Y. Silberberg, *Science* **328**, 879 (2010).
- [8] M. D'Angelo, M. V. Chekhova, and Y. Shih, *Phys. Rev. Lett.* **87**, 013602 (2001).
- [9] Y. Kawabe, H. Fujiwara, R. Okamoto, K. Sasaki, and S. Takeuchi, *Opt. Express* **15**, 14244 (2007).
- [10] H. J. Chang, H. Shin, M. N. O'Sullivan-Hale, and R. W. Boyd, *J. Mod. Opt.* **53**, 2271 (2006).
- [11] J. Gea-Banacloche, *Phys. Rev. Lett.* **62**, 1603 (1989); J. Javanainen and P. L. Gould, *Phys. Rev. A* **41**, 5088 (1990); D.-I. Lee and T. Goodson III, *J. Phys. Chem. B Lett.* **110**, 25582 (2006).
- [12] O. Steuernagel, *J. Opt. B: Quantum Semiclass. Opt.* **6**, S606 (2004).
- [13] M. Tsang, *Phys. Rev. A* **75**, 043813 (2007).
- [14] M. Tsang, *Phys. Rev. Lett.* **101**, 033602 (2008).
- [15] W. N. Plick, C. F. Wildfeuer, P. M. Anisimov, and J. P. Dowling, *Phys. Rev. A* **80**, 063825 (2009).
- [16] M. Tsang, *Phys. Rev. Lett.* **102**, 253601 (2009).
- [17] G. Goltzman *et al.* *Appl. Phys. Lett.* **79**, 705 (2001)
- [18] B. Dayan, A. Peer, A. A. Friesem, and Y. Silberberg, *Phys. Rev. Lett.* **94**, 043602 (2005)